Ciência Rural, Santa Maria, v.53:6, e20210893, 2023
http://doi.org/10.1590/0103-8478cr20210893
ISSNe 1678-4596
CLINIC AND SURGERY

Finite element analysis of a new intervertebral disc prosthesis developed for the canine cervical spine

Paulo Vinícius Tertuliano Marinho[1*] **Ana Paula Macedo**[2] **Cláudio Pereira de Sampaio**[3] **Antônio Carlos Shimano**[4] **Carolina Camargo Zani Marinho**[1] **Mônica Vicky Bahr Arias**[5]

[1]Departamento de Medicina Veterinária, Instituto Federal de Educação, Ciência e Tecnologia do Sul de Minas Gerais (IFSULDEMINAS), 37890-000, Muzambinho, MG, Brasil. E-mail: paulo.marinho@muz.ifsuldeminas.edu.br. *Corresponding author.
[2]Departamento de Materiais Dentários e Prótese, Faculdade de Odontologia de Ribeirão Preto, Universidade de São Paulo (USP), Ribeirão Preto, SP, Brasil.
[3]Departamento de Design, Universidade Estadual de Londrina (UEL), Londrina, PR, Brasil.
[4]Faculdade de Medicina de Ribeirão Preto, Universidade de São Paulo, Departamento de Ortopedia e Anestesiologia, Ribeirão Preto, SP, Brasil.
[5]Departamento de Medicina Veterinária, Universidade Estadual de Londrina (UEL), Londrina, PR, Brasil.

ABSTRACT: Cervical spondylomyelopathy (CSM) is a disease that affects mostly large- and giant-breed dogs. It is characterized by abnormalities of the cervical spine that may cause damage to the spinal cord and nerve roots. Cervical disc arthroplasty has been proposed as a treatment option in veterinary medicine. The current study evaluated the main stresses in a novel canine vertebral disc prosthesis and vertebral bodies using finite element analysis. Two experimental groups were created based on the material used for the prosthesis: stainless steel group (SSG) and titanium alloy group (TAG). Vertebral and prosthetic average equivalents von-Mises stress (VMS) and minimum principal stress (MiPS) were assessed while compressive, tensile, and lateral bending shear loads were applied. The stainless steel group had greater VMS distribution on all the evaluated parameters while the titanium alloy group had greater MiPS. Stresses were more concentrated on the lateral and ventral surfaces of the vertebral bodies than on their endplates. The average prosthetic stresses were more concentrated on the bone/implant contact surface than on the prosthesis/screw interface. Maximum stresses were concentrated in the screws' cranial surface. The novel prosthesis allows even distribution along the vertebral body. Comparing prosthesis materials, titanium alloy was marginally superior regarding average stresses in all directions and should be less likely to suffer subsidence.
Key words: finite element model, canine, vertebrae, novel implant, arthroplasty.

Elementos finitos de uma nova prótese de disco intervertebral desenvolvida para a coluna cervical canina

RESUMO: Espondilomielopatia cervical (EMC) é uma doença que geralmente afeta cães de raças grandes e gigantes. Ela é caracterizada por anormalidades da coluna cervical que podem causar danos à medula espinhal ou às raízes nervosas. Artroplastia cervical com prótese de disco tem sido proposta como opção de tratamento na medicina veterinária. O presente estudo teve como objetivo avaliar os principais estresses em uma nova prótese de disco intervertebral canina e corpos vertebrais por meio da análise de elementos finitos. Foram compostos dois grupos experimentais que representaram o material constituinte da nova prótese: grupos aço inoxidável (SSG) e o liga de titânio (TAG). Tensões equivalente de von-Mises (VMS) e tensão principal mínima (MiPS) média foram avaliadas sob forças de compressão, tração e torção para vértebras e prótese. O grupo SSG teve maior distribuição de VMS para todos parâmetros avaliados, enquanto o grupo TAG teve maior MiPS. Estresses estiveram mais concentrados nas superfícies lateral e ventral dos corpos vertebrais do que nas placas terminais. Os estresses médios da prótese foram mais concentrados na superfície de contato osso/implante do que na interface prótese/parafuso. Estresses máximos foram concentrados na superfície cranial do parafuso. A nova prótese permitiu distribuição uniforme do estresse ao longo do corpo vertebral. Comparando os materiais da prótese, a liga de titânio foi marginalmente superior quanto aos estresses médios em todas as direções, sendo menos provável que sofra afundamento da prótese.
Palavras-chave: modelo de elementos finitos, canino, vértebra, novo implante, artroplastia.

INTRODUCTION

Cervical spondylomyelopathy (CSM) is a disease that affects mainly large- and giant-breed dogs, characterized by abnormalities of the cervical spine that may cause dynamic and static compressions of the spinal cord and/or nerve roots (ADAMO et al., 2007; DA COSTA, 2010).

Vertebral distraction-fusion techniques are well established surgical treatments that aim to

Received 12.21.21 Approved 07.26.22 Returned by the author 09.19.22
CR-2021-0893.R1
Editors: Rudi Weiblen Alexandre Mazzanti

distract and stabilize the vertebrae to eliminate the dynamic compression component (DA COSTA, 2010; SEIM, 2008). These techniques provide good results; however, they can cause biomechanical changes and increase motion at the adjacent intervertebral spaces. That consequently raises intradiscal pressure and results in degeneration of the cranial and caudal intervertebral discs in the so-called adjacent segment disease (ECK et al., 2002).

A cervical arthroplasty technique (Adamo Spinal Disc, Applied Veterinary Technology, Walnut Creek, Calif) (DA COSTA, 2010; ADAMO, 2011; ADAMO et al., 2014a) was proposed for dogs with disc-associated CSM. This technique preserved the vertebral range of motion while providing distraction and stability, so complete spinal cord decompression can be achieved (DA COSTA, 2010; ADAMO, 2011).

Some authors have reported good to excellent outcome in most dogs that underwent cervical arthroplasty surgery. The technique has shown effectiveness on providing vertebral distraction and preserving segmental motion; although, complications like loss of vertebral distraction and vertebral instability occurred over time (ADAMO et al., 2014a; ADAMO et al., 2014b).

One of the most commonly reported complications following intervertebral disc arthroplasty in people is subsidence (GOFFIN et al., 2002; VAN LOON & GOFFIN, 2012). It is most often caused by inadequate preoperative planning and/or inaccurate bone density assessment, but it can also be a consequence of improper prosthetic design with misdistribution of stresses from the artificial cervical devices to the vertebral end plates (VAN LOON & GOFFIN, 2012).

The current study created a finite element model of a novel intervertebral disc prosthesis for the canine cervical spine, and predicted stress patterns at bone-implant interfaces at C5–C6 levels for two different prosthetic materials.

MATERIALS AND METHODS

Prosthesis

The *PVTM Cervical Disc* prosthesis (patent registration number: BR10201403025), combines an intervertebral spacer with a conventional screw fixation mechanism that is contained within the excised disc space. Dimensions of the prosthesis were based on previous cadaveric studies of sixteen cervical (C5-C6) functional spinal units (FSUs) collected from skeletally mature mixed-breed dog cadavers with body weight ranging from 25 to 35 kg (Table 1). Each part of the prosthesis (P1 and P2) has a vertical and a horizontal plate (Figure 1A). P1 is angled at 71º and P2 is angled at 110º to fit perfectly in each vertebra (Figure 1C). The contact surface has a support bracket (rib) (Figure 1B) that increases the implant's strength and can be fixed to the vertebral bodies with 2.7 x 12 mm locking screws (Figure 1C e D). A 3.7 mm ball-and-socket shape is used to preserve physiologic vertebral motion. The prosthesis can move 12º in extension, 25º in lateral bending and 18º in flexion.

Finite element analysis

The prothesis design was imported into Ansys Workbench® (Swanson Analysis Systems, Inc., Houston, USA). Two groups were created for FEM simulation to analyze the behavior of two different prosthesis materials: stainless steel group (SSG) and titanium alloy group (TAG).

Stress distribution was assessed in each vertebral body under normal physiologic loads in maximum ventral flexion, extension, and lateral bending. Stresses were measured at the vertebral body/implant interface, at the cranial (P1) and caudal parts (P2) of the prostheses and at the screw/implant interface. Finite element analysis was divided into pre-processing, solution, and post-processing phases.

Table 1 - Dimensions (in milimeters) of the main structural parts of the PVTM Cervical Disc prosthesis.

-------------------------------------Structure of the prosthesis------------------------------------		Dimensions (mm)
P1	Vertical plate	17
	Horizontal plate	29
	Width of the vertical plate	17
P2	Vertical plate	15
	Horizontal plate	20
	Width of the vertical plate	17

Pre-processing

The designed vertebrae and prostheses models were exported to the software Ansys Workbench® 10.0 (Swanson Analysis Systems, Inc., Houston, USA). Specific materials properties (elasticity modulus/Young and Poisson's ratio) were also included in the software (Table 2).

The finite element mesh was then generated (Figure 2). The mesh subdivided the geometry into elements and nodes. This mesh was composed of 70.573 elements and 110.696 nodes. Elements SOLID187 and SOLID186 were used for solid elements, and elements CONTA174 and TARGE170 were used for the contact. The mesh was refined until the results converged, even with decreased element size.

All materials were considered homogeneous and isotropic. Therefore, each set element was characterized by specifying the type of material within the software. After the elements were characterized, boundary conditions (attachment points and movement restrictions), and loads were applied. The type of contact between the models in the finite element program was considered glued/perfect, so there was no coefficient of friction in the bone/implant interface.

Solution

After all properties were determined and loads were applied, equations were assembled into matrix form and solved numerically.

Loads were applied at the craniolateral, craniodorsal, and cranioventral portions of C5 vertebral body. The vertebral body of C6 was restrained from movement, and a 50 N force (ADAMO et al., 2007) was applied to C5 in maximum extension, lateral bending, and flexion in both groups (Figure 3). These were the chosen boundary conditions.

The *solver tool* of Ansys Workbench® 10.0 was used to obtain a solution (MACEDO et al., 2015; TONIOLLO et al., 2017). Mean simulation time was 3 hours for each specimen.

Post-processing

After the mesh was prepared and checked, boundary conditions were applied, and the model was solved, the results were analyzed for each group. Average values for von-Mises stresses (VMS) and Minimum Principal Stress (MiPS) were assessed in the *PVTM Cervical Disc* and at the bone/implant interface, under normal physiologic loads in flexion, extension, and lateral bending.

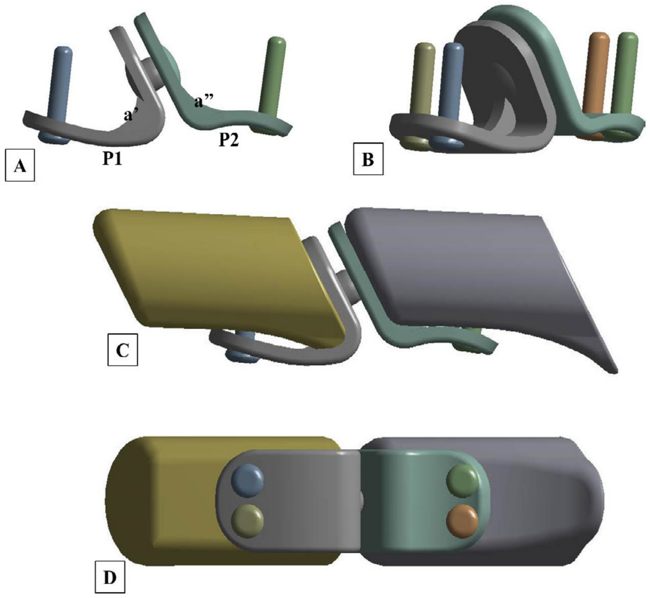

Figure 1 - Finite element model of the *PVTM Cervical Disc* prosthesis interposed between C5-C6 (A); finite element model of the PVTM Cervical Disc prosthesis represented by the cranial part, caudal part, and screws (B) (P1: cranial part of the prostheses; P2: caudal part (P2) of the prostheses; a': support bracket of the cranial part of the prostheses).

Table 2 - Mechanical property values for each structure.

Structure	Elasticity modulus / Young (MPa)	Poisson's ratio	Reference
Titanium alloy	114 x 10^3	0.30	MONTEITH, 1993; ÇIFTÇI & CANAY, 2000; PIERRISNARD et al., 2003
Steel	200 x 10^3	0.30	KO et al., 1992; SERTGÖZ, 1997
Cancellous bone	100	0.20	KO et al., 1992; SERTGÖZ, 1997
Cortical bone	12000	0.30	KO et al., 1992; SERTGÖZ, 1997

Von-Mises stresses generated in the ductile structures [steel and titanium prosthesis (P1, P2, screws)] and on the non-ductile structures (bone) was previewed and recorded in Megapascal (MPa). Minimum Principal Stress generated in the non-ductile structures (bone) was previewed and recorded, also in Megapascal (MPa). All generated stresses were previewed on color scale, where each shade corresponded to a different stress intensity.

Four vertebral body surfaces were included in the simulation [lateral (left side) and ventral surfaces (C5 e C6), C5 caudal endplate and C6 cranial endplate]. Two screw surfaces were included in the simulation [cranial (considering the four screws) and caudal (considering the four screws)]. To develop the prosthesis, eight surfaces were included (four on P1 and four on P2): the caudal and cranial surfaces of the vertical plate, and the dorsal and ventral surfaces of the horizontal plate. The average stress generated in each frame during the test was then calculated.

Statistical analysis

Descriptive statistics were performed using the length measurements. Numerical instability of the FEM was verified by the decrease in element size and the mesh refinement. The solution was considered converged when the variation of the sequential analytical results was less than 3% (MELLO, 2004).

RESULTS

FEM analysis

Von-Mises stresses on the vertebral body was lower than on the prosthesis in both groups (Table 3). The

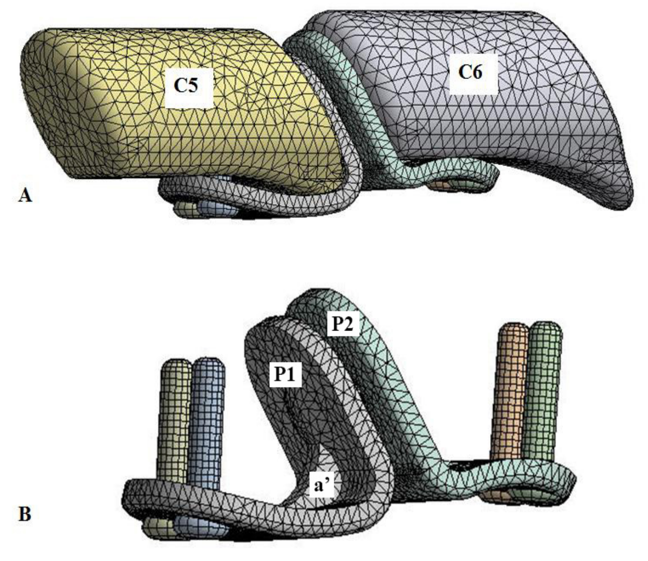

Figure 2 - Functional spinal model C5-C6 in a neutral position during application of 50 N to the endplate of C5 after maximum extension (A), lateral bending (B) and flexion (C).

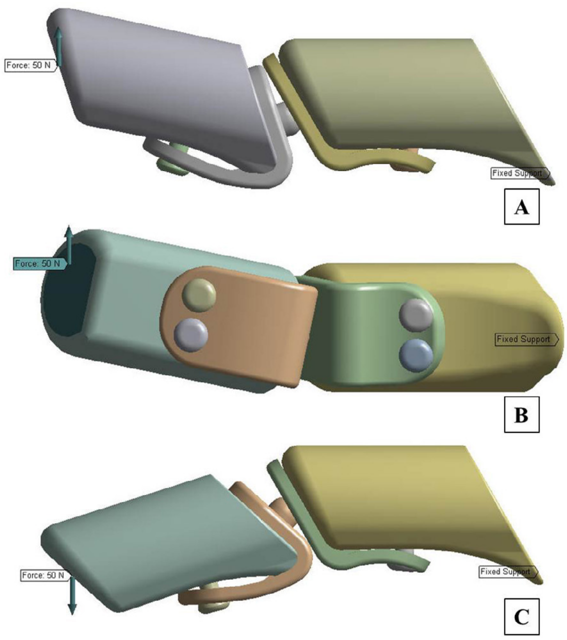

Figure 3 - Model of the PVTM Cervical Disc prosthesis A. lateral view; B. Final design in 3D; C. prosthesis interposed between C5-C6; D. prosthesis interposed between C5-C6; E. Ventral view. (P1: cranial part of the prostheses; P2: caudal part (P2) of the prostheses; a’: support bracket of the cranial part of the prostheses; a”: support bracket of the caudal part of the prostheses).

stainless steel group had greater VMS in all structures compared to the titanium alloy group (Table 3). Von-Mises stresses predicted at the vertebral bodies was greater at the lateral and ventral surfaces than at the end plates in both groups (Figures 4, 5, 6 and 7).

Stress level for P1 was higher at the caudal surface of the vertical plate for both groups. Stress level for P2 was higher at the ventral surface of the horizontal plate. Tension was reported only on contact surfaces, mainly on the convex part of the ball-and-socket design. There was incremental stress during extension and lateral bending and flexion on the dorsal, lateral and ventral edges of the caudal surface of the vertical plate of P1 and on the cranial surface of the vertical plate of P2 (Figures 4, 5, 6 and 7). The evaluation of equivalent VMS on the surfaces of the screw was higher on the cranial portion of the screw, especially on the screw-interface horizontal plate.

Quantitative evaluation of MiPS was similar in both groups (Table 4); however, in the

Table 3 - Average equivalent von-Mises stress (VMS) on bone, P1, P2 and screws after loads were applied for stainless steel group (SSG) and titanium alloy group (TAG).

Applied force	--------Evaluated structure--------							
	------Vertebral body------		--------P1--------		--------P2--------		------Screws------	
	SSG	TAG	SSG	TAG	SSG	TAG	SSG	TAG
Extension	2.6	2.5	247.5	187.5	262.5	187.5	225.0	150.0
Lateral bending	2.5	2.1	187.5	157.5	270.0	232.5	250.0	252.3
Flexion	2.2	1.9	187.5	165.0	172.5	135.0	133.0	91.7
Total average	2.4	2.2	207.5	170.0	235.0	185.0	202.7	164.6

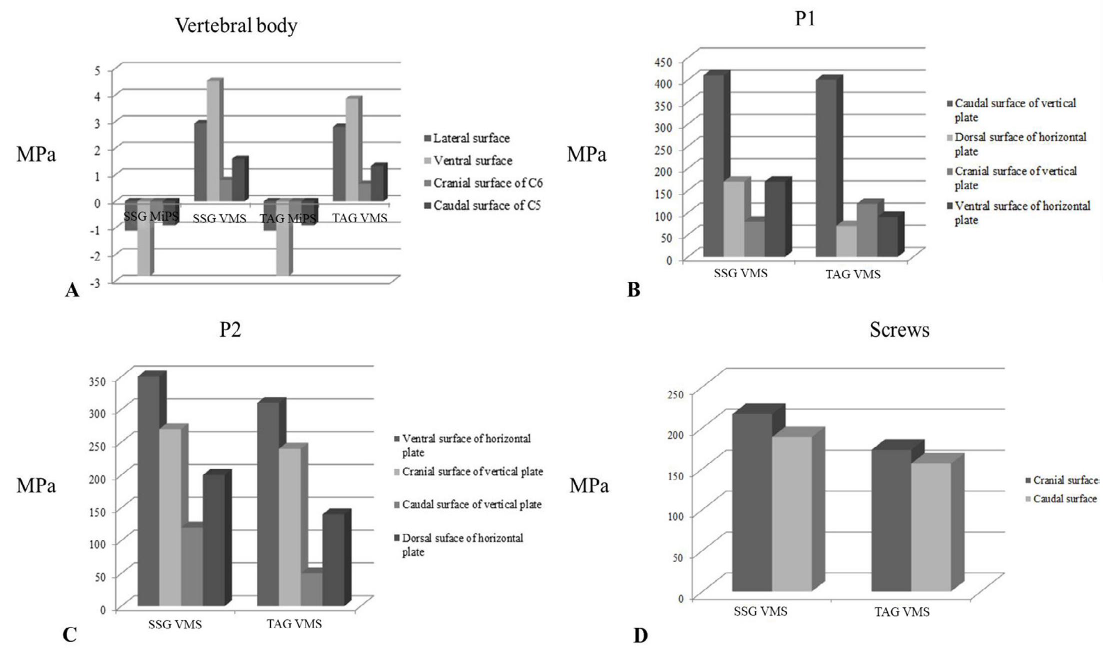

Figure 4 - Average equivalent von-Mises stress (VMS) and minimum principal stress (MiPS) on the bone surface (A); average equivalent VMS in P1 (B), P2 (C), and screws (D) under maximum extension, lateral bending and flexion for stainless steel group (SSG) and titanium alloy group (TAG).

qualitative evaluation, MiPS was concentrated in more regions in group TAG (Figures 5, 6 and 7).

DISCUSSION

The 14% (ADAMO et al., 2014b) to 92% (FALZONE et al., 2022) complication rate of late prosthesis subsidence the currently commercially available canine cervical prostheses led the authors to assess a new cervical disc prosthesis. This novel implant allows for adequate fixation onto the vertebral body with additional screw fixation to hold the device in position and homogeneous distribution of Von-Mises stresses and MiPS along the vertebral body, and does not overload the endplates.

Von-Mises stresses represent the average of stresses in all directions. Conversely, MiPS is negative and represents the maximum compression of the analysis area, whereas determining those normal peak values in the implant system and in the tissue can provide valuable information with respect to potential fracture sites and bone atrophy.

Stresses on C6 and C5 endplates were lower than on other surfaces in both groups. This reduces the risk of subsidence, which occurs when a structure with a high modulus of elasticity, such as the device, penetrates another structure with a low modulus of elasticity, such as the vertebral body. The magnitude of subsidence is directly proportional to the load pressure and to the difference between the elasticity modules but inversely proportional to the area of the graft–bed interface (PINDER & SHARP, 2016). Good results were reported with the use of stainless steel sphere implants; however, a reduction in disc height occurred secondary to sphere subsidence into the endplates because the contact point between the ball and the surface of the vertebra was too small and stresses concentrated on a single point (LINK et al., 2004). In humans, subsidence is the most commonly reported device-related complication in intervertebral disc arthroplasty. It can be attributed to a deficiency in endplate preparation, inadequate prosthesis design, and osteopenia or metabolic bone disease resulting in decreased bone quality (ANDERSON & ROULEAU, 2004). The contact area of the only commercially available canine cervical disk prosthesis (Adamo Spinal Disc, Applied Veterinary Technology, Walnut Creek, Calif) has not been evaluated, but appears to be relatively small compared with the surface area of a cervical end plate, and subsidence of the prosthesis has been reported (ADAMO et al., 2014b). The *PVTM Cervical Disc* may have a greater distribution of forces due to a larger

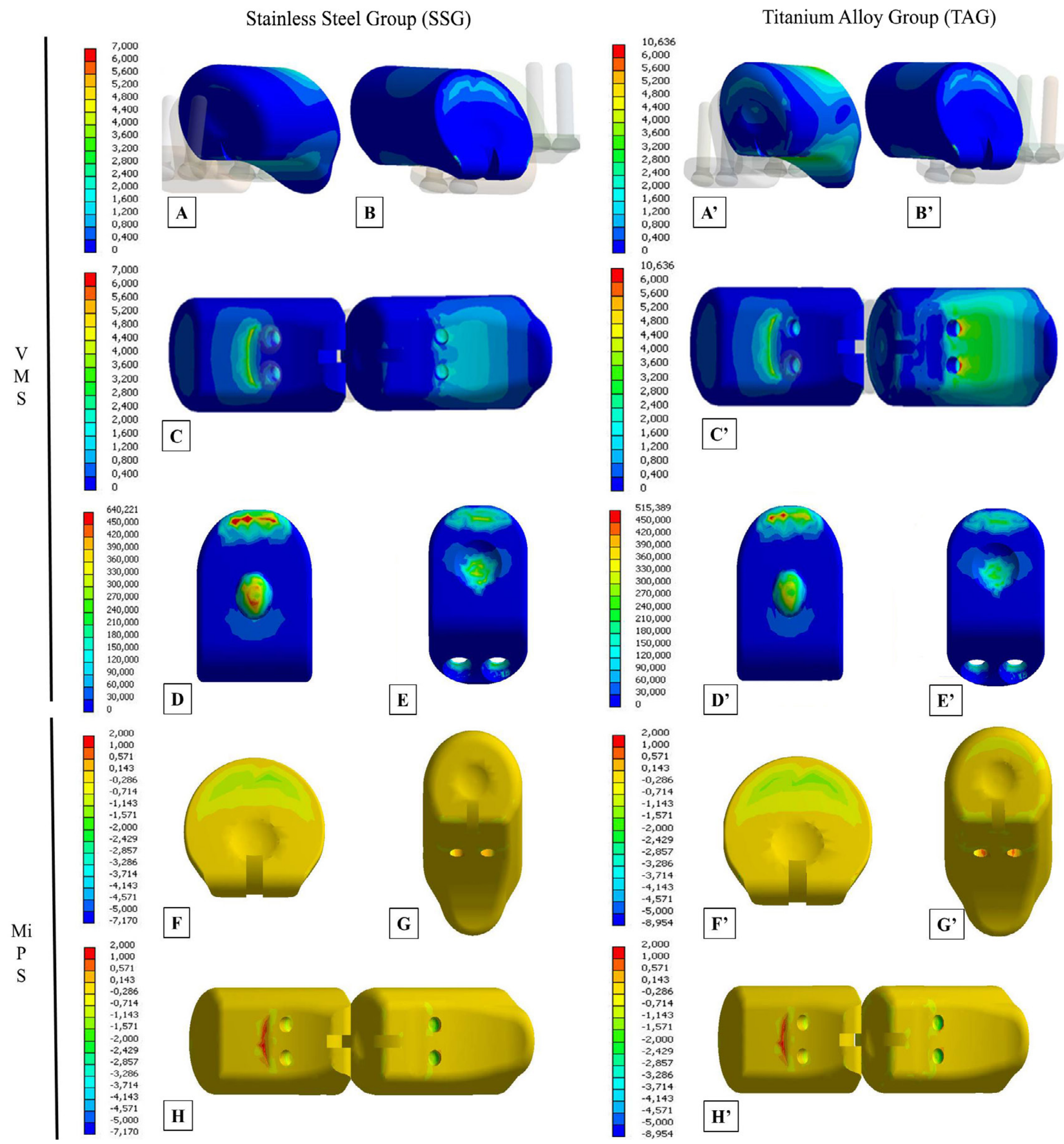

Figure 5 - Quantitative and qualitative assessment of the stresses on the main surfaces after applying extension forces. Average equivalent von-Mises stress (VMS) on the cranial endplate of C6 (A, A'), caudal endplate of C5 (B, B'), ventral surface of C5 and C6 (C, C'), caudal surface of the vertical plate of P1 (D, D'), and cranial surface of the vertical plate of P2 (E, E'). Minimum principal stress (MiPS) on the cranial endplate of C6 (F, F'), caudal endplate of C5 (G, G'), and ventral surface of C5 and C6 (H, H') for stainless steel group (SSG) and titanium alloy group (TAG).

contact surface at the endplate and homogeneous distribution of tension between the endplates and the bone-screw interface.

The largest VMS were detected in P1, P2, and screws in the SSG, meaning that more rigid material such as stainless steel induces higher magnitudes of stresses than less rigid material (titanium alloy) (KO et al., 1992; SERTGÖZ, 1997). When comparing the stress obtained at the vertebral bodies, the results were similar; however, there were higher stress values for the stainless steel model, possibly because their elasticity modulus is larger than the titanium alloy (PHILLIPS & GARFIN, 2005; SEKHON et al., 2007). Higher compressive stress was observed in more regions of the vertebral body in the TAG compared to the SSG. This indicate that a higher modulus of elasticity and subsequent subsidence of the

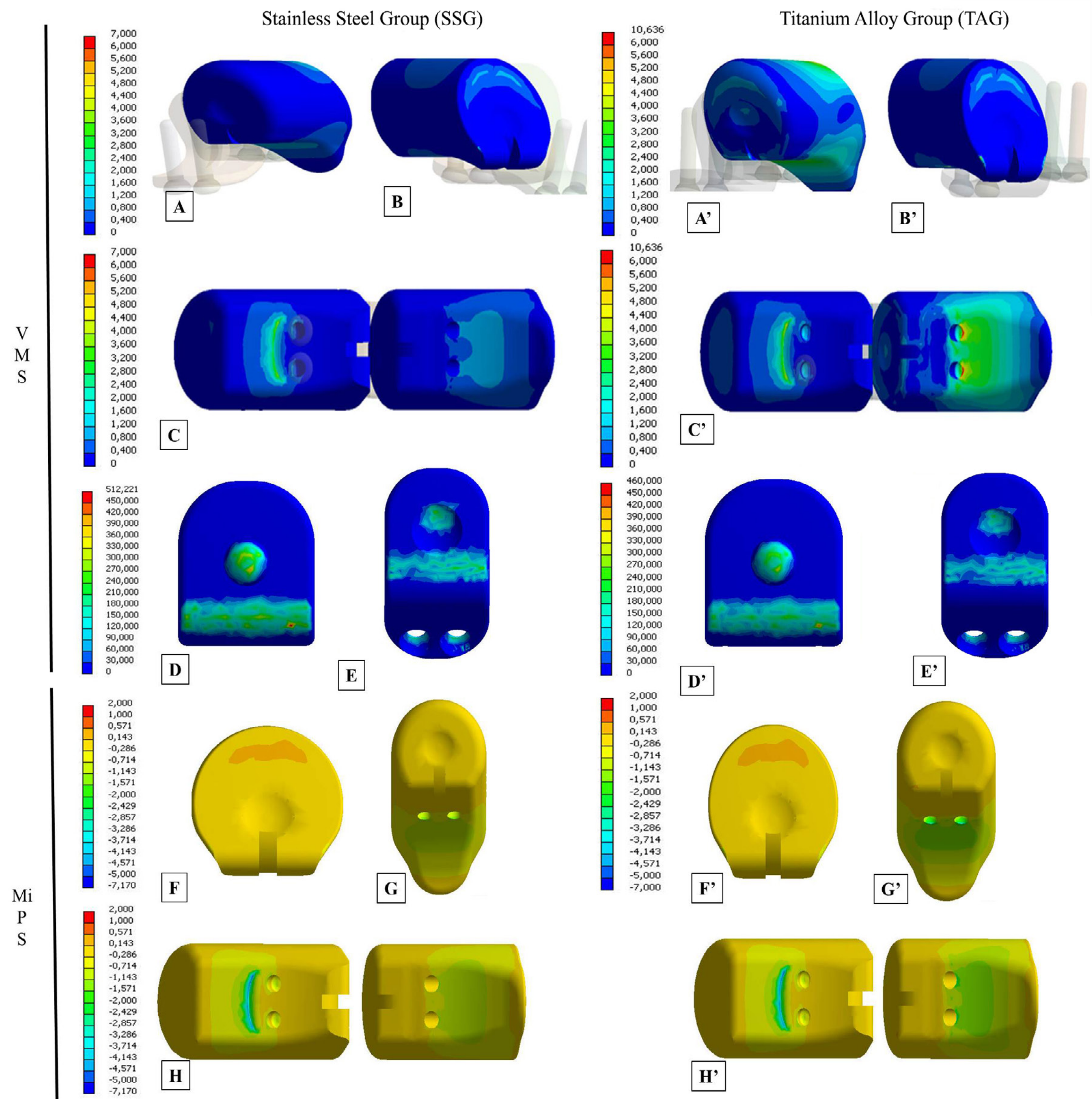

Figure 6 - Quantitative and qualitative assessment of the stresses exerted on the main surfaces after flexion. Average equivalent von-Mises stress (VMS) in the cranial endplate of C6 (A, A'), caudal endplate of C5 (B, B'), ventral surface of C5 and C6 (C, C'), caudal surface of the vertical plate P1 (D, D'), and cranial surface of the vertical plate P2 (E, E'). Minimum principal stress (MiPS) on the cranial endplate of C6 (F, F'), caudal endplate of C5 (G, G'), and ventral surface of C5 and C6 (H, H') for stainless steel group (SSG) and titanium alloy group (TAG).

prosthesis may have a stronger correlation with the average forces acting on the bone (VMS) than with only the compressive stresses (MiPs).

The higher stress values reported on the lateral and ventral surface of the vertebral body are likely a result of anchoring the *PVTM Cervical Disc* in the vertebral bodies using screws. This distributes the stress more homogeneously, resulting in greater tension in limited and specific points of the ventral surface of the vertebral body. The idea is to distribute the forces involved as evenly as possible over a large area (LINK et al., 2014). The interface between the implant and the vertebra allow transmission of axial forces between adjacent vertebrae (SEKHON, 2005). In addition to allowing greater distribution of stress along the lateral and ventral surface of the vertebral bodies to preserve the C5 and

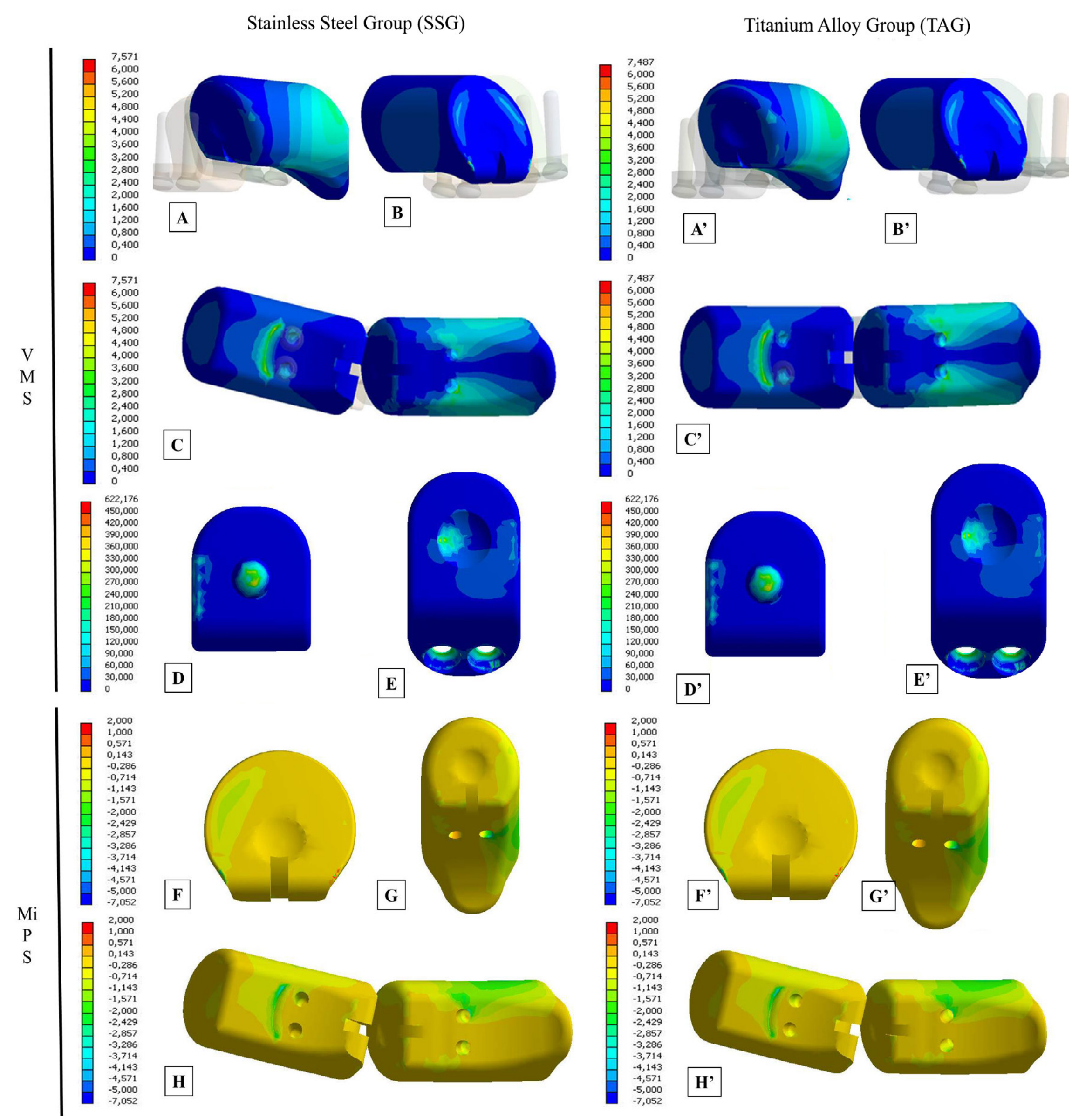

Figure 7 - Quantitative and qualitative assessment of stresses on the main surfaces after lateral bending. Average equivalent von-Mises stress (VMS) on the cranial endplate of C6 (A, A '), caudal endplate of C5 (B, B'), ventral surface of C5 and C6 (C, C '), caudal surface of the vertical plate P1 (D, D'), and cranial surface of the vertical plate P2 (E, E'). Minimum principal stress (MiPS) on the cranial endplate of C6 (F, F'), caudal endplate of C5 (G, G'), and ventral surface of C5 and C6 (H, H') for stainless steel group (SSG) and titanium alloy group (TAG).

C6 endplates, fixation screws are intended to prevent loosening and migration of the prosthesis as described by some authors using the Bryan Disc® (Medtronic Sofamor Danek, Memphis, USA) in people (GOFFIN et al., 2002; VAN LOON & GOFFIN, 2012) while better distributing stresses along various parts of the prosthesis (BEAURAIN et al., 2009; WIGFIELD et al., 2002).

The developed prosthesis resembles the Prestige ST (Medtronic Sofamor Danek, Memphis, Tennessee, USA), that is inserted into the disc space and fixed to the vertebral bodies by bone screws (TRAYNELIS, 2005). This prosthesis in humans was effective in maintaining movement four years after surgery (ROBERTSON & METCALF, 2004).

Table 4 - Average minimum principal stress (MiPS) on bone after applying extension, flexion and lateral bending forces for stainless steel group (SSG) and titanium alloy group (TAG).

Applied force	--Evaluated structure----------------------------------	
	---Vertebral body---------------------------------------	
	SSG	TAG
Extension	-1.1	-1.1
Lateral bending	-1.3	-1.3
Flexion	-2.05	-2.05
Total average	-1.4	-1.4

A specific point that virtually received no stress during the application of strength onto the *PVTM Cervical Disc* prosthesis was the transition between the vertical and caudal plates in both P1 and P2, which possibly eliminates the importance of placing a rib to obtain resistance at that point. There were no bending forces between the vertical and horizontal plates during load application.

Individual assessment of P1 areas in SSG and TAG showed that the caudal surface of the vertical plate and the convex part of the ball-and-socket design received higher magnitudes of stress than other surfaces, maybe because the caudal surface of P1 vertical plates in both groups is in direct contact with the cranial surface of P2 vertical plates. The metal-metal contact exacerbated the stress on these points, increasing friction during extension, lateral bending, and flexion. Studies on cervical devices observed that the core of the prosthesis is the most stressed component during axial compression and compression/shear (MUMMANENI et al., 2007; CAMPELLO et al., 2009). The distribution of stresses on the cranial surface of the P2 vertical plate is also explained by the lack of a shock-absorber on the metal contact surfaces. The application of forces after lateral bending, flexion and maximum extension was very important to assess specific points of stress on the edges of the prosthesis plates.

The results allow for a better understanding of the potential locations of stress but have some limitations. In the FE model, the loads are controlled, and the effects of other spinal structures such as muscles and ligaments are not considered. Another limitation is that the contact was considered perfect in the FE analysis, but the coefficient of friction between the two parts of the prostheses was not considered. Knowledge of the behavior of biomedical devices under cyclic loads is fundamental because cyclic fatigue in the implanted materials is one of the most critical failures observed in cervical disc prosthesis (CAMPELLO et al., 2009). Therefore, additional biomechanical and long-term follow-up studies are needed to properly assess the biomechanics and safety of this type of device (BARBIER et al., 1998).

CONCLUSION

The *PVTM Cervical Disc* prosthesis had a homogeneous distribution of stresses throughout the vertebral body, with reduced stress on the vertebral endplates, which could possibly prevent subsidence and subsequent decrease of distraction and intervertebral mobility. Comparing the prosthesis materials, titanium alloy was marginally superior regarding average stresses in all directions and should be less likely to suffer subsidence.

ACKNOWLEDGEMENTS

The authors thank the Conselho Nacional de Desenvolvimento Científico e Tecnológico (CNPQ), Brasil for granting a Master scholarship in Animal Science to the corresponding author and the Coordenação de Aperfeiçoamento de Pessoal de Nível Superior (CAPES), Brasil – Finance code 001, for their financial support. Special thanks should be given to Henrique Eduardo Vilela Oliveira (Veterinary Resident at Londrina State University, Londrina-PR, Brazil) for his immense contribution in facilitating the collection and dissection of the cervical vertebral columns used in this study.

DECLARATION OF CONFLICT OF INTEREST

The PVTM Cervical Disc implant was designed Dr. Paulo Vinícius Tertuliano Marinho.

BIOETHICS AND BIOSECURITY COMMITTEE APPROVAL

The study was approved by the Londrina State University Ethics Committee on Animal Use (CEUA-UEL) under protocol 155/2013 according to the Brazilian Government principles for the utilization and care of vertebrate animals.

AUTHORS' CONTRIBUTIONS

All authors contributed equally for the conception and writing of the manuscript. All authors critically revised the manuscript and approved of the final version.

REFERENCES

ADAMO, P. F. et al. Cervical disc arthroplasty using the Adamo Spinal Disc® in 30 dogs affected by disc associated wobbler syndrome at single and multiple levels. **Journal of Veterinary Internal Medicine**, v.28, n.3, p.949–950, 2014. Available from: <https://doi.org/10.1111/jvim.12323>. Accessed: Dec. 12, 2021. doi: 10.1111/jvim.12323.

ADAMO, P. F. et al. Cervical disc arthroplasty in dogs with disc associated wobbler syndrome – limitations and how to prevent possible complications. **Journal of Veterinary Internal Medicine**, v.28, n.3, p.1357, 2014. Available from: <https://doi.org/10.1111/jvim.12323>. Accessed: Dec. 12, 2021. doi: 10.1111/jvim.12323.

ADAMO, P. F. et al. In vitro biomechanical comparison of cervical disk arthroplasty, ventral slot procedure, and smooth pins with polymethylmethacrylate fixation at treated and adjacent canine cervical motion units. **Veterinary Surgery**, v.36, n.8, p.729–741, 2007. Available from: <https://doi.org/10.1111/j.1532-950X.2007.00327.x>. Accessed: Dec. 12, 2021. doi: 10.1111/j.1532-950X.2007.00327.x.

ADAMO, P. F. Cervical arthroplasty in two dogs with disk-associated cervical spondylomyelopathy. **Journal of the American Veterinary Medical Association**, v.239, n.6, p.808–817, 2011. Available from: <https://doi.org/10.2460/javma.239.6.808>. Accessed: Dec. 12, 2021. doi: 10.2460/javma.239.6.808.

ANDERSON, P. A.; ROULEAU, J. P. Intervertebral disc arthroplasty. **Spine**, v.29, n.23, p.2779–2786, 2004. Available from: <https://doi.org/10.1097/01.brs.0000146460.11591.8a>. Accessed: Dec. 12, 2021. doi: 10.1097/01.brs.0000146460.11591.8a.

BARBIER, L. et al. Finite element analysis of non-axial versus axial loading of oral implants in the mandible of the dog. **Journal of Oral Rehabilitation**, v.25, n.11, p.847–858, 1998. Available from: <https://doi.org/10.1046/j.1365-2842.1998.00318.x>. Accessed: Dec. 12, 2021. doi: 10.1046/j.1365-2842.1998.00318.x.

BEAURAIN, J. et al. Intermediate clinical and radiological results of cervical TDR (Mobi-C) with up to 2 years of follow-up. **European Spine Journal**. v.18, n.6, p.841–850, 2009. Available from: <https://doi.org/10.1007/s00586-009-1017-6>. Accessed: Dec. 12, 2021. doi: 10.1007/s00586-009-1017-6.

CAMPELLO, T. N. et al. Prótese para substituição total de disco intervertebral: Desenvolvimento de modelo computacional e análise por elementos finitos. **Coluna/ Columna**, v.8, n.1, p.38–42, 2009. Available from: <https://doi.org/10.1590/S1808-18512009000100008>. Accessed: Dec. 12, 2021. doi: 10.1590/S1808-18512009000100008.

ÇIFTÇI, Y.; CANAY, S. The effect of veneering materials on stress distribution in implant-supported fixed prosthetic restorations. **The International Journal of Oral & Maxillofacial Implants**, v.15, n.4, p.571–582, 2000. Available from: <http://medlib.yu.ac.kr/eur_j_oph/ijom/IJOMI/ijomi_15_571.pdf>. Accessed: Dec. 12, 2021.

DA COSTA, R. C. Cervical spondylomyelopathy (Wobbler Syndrome) in dogs. **The Veterinary Clinics of North America. Small Animal Practice**, v.40, n.5, p.881–913, 2010. Available from: <https://doi.org/10.1016/j.cvsm.2010.06.003>. Accessed: Dec. 12, 2021. doi: 10.1016/j.cvsm.2010.06.003.

FALZONE, C. et al. Comparison of two surgical techniques for the treatment of canine disc associated-cervical spondylomyelopathy. **Frontiers in Veterinary Science**, v.9, p.1-12, 2022. Available from: <https://doi.org/10.3389/fvets.2022.880018>. Accessed: Jun. 23, 2022. doi: 10.3389/fvets.2022.880018.

GOFFIN, J. et al. Preliminary clinical experience with the bryan cervical disc prosthesis. **Neurosurgery**, v.51, n.3, p.840–847, 2002. Available from: <https://doi.org/10.1227/00006123-200209000-00048>. Accessed: Dec. 12, 2021. doi: 10.1227/00006123-200209000-00048.

KO, C. C. et al. Micromechanics of implant/ tissue interfaces. **The Journal of Oral Implantology**, v.18, n.3, p.220–230, 1992.

LINK et al. Choosing a cervical disc replacement. **The Spine Journal**. v.4, n.6 Suppl, p.294S–302S, 2004. Available from: <https://doi.org/10.1016/j.spinee.2004.07.022>. Accessed: Dec. 12, 2021. doi: 10.1016/j.spinee.2004.07.022.

MACEDO, A. P. et al. Biomechanical evaluation of a spinal screw system by the finite element method. **International Journal of Morphology**, v.33. n.1, p.318-326, 2015. Available from: <https://doi.org/10.4067/S0717-95022015000100050>. Accessed: Jun. 19, 2021. doi: 10.4067/S0717-95022015000100050.

MELLO, G. M. R. **Efeito de elementos betagênicos na estabilidade de fases e propriedades de ligas de titânio para implantes ortopédicos**. 2004. 113f. Thesis (Doctorate in Mechanical Engineering) – Course of Mechanical Engineering, Campinas State University.

MONTEITH, B. D. Minimizing biomechanical overload in implant prostheses: A computerized aid to design. **The Journal of Prosthetic Dentistry**, v.69, n.93, p.495–502, 1993. Available from: <https://doi.org/10.1016/0022-3913(93)90159-l>. Accessed: Dec. 12, 2021. doi:10.1016/0022-3913(93)90159-l.

MUMMANENI, P. V. et al. Cervical arthroplasty with the PRESTIGE LP cervical disc. **Neurosurgery**, v.60, n.4 Suppl 2, p.310–315, 2007. Available from: <https://doi.org/10.1227/01.NEU.0000255376.42099.13>. Accessed: Dec. 12, 2021. doi: 10.1227/01.NEU.0000255376.42099.13.

PHILLIPS, F. M.; GARFIN, S. R. Cervical disc replacement. **Spine**. v.30, n.17 Suppl, p.S27-S33, 2005. Available from: <https://doi.org/10.1097/01.brs.0000175192.55139.69>. Accessed: Dec. 12, 2021. doi:10.1097/01.brs.0000175192.55139.69.

PIERRISNARD, L. et al. Influence of implant length and bicortical anchorage on implant stress distribution. **Clinical Implant Dentistry and Related Research**. v.5, n.4, p.254–262, 2003. Available from: <https://doi.org/10.1111/j.1708-8208.2003.tb00208.x>. Accessed: Dec. 12, 2021. doi: 10.1111/j.1708-8208.2003.tb00208.x.

PINDER, E. M.; SHARP, D. J. Cage subsidence after anterior cervical discectomy and fusion using a cage alone or combined with anterior plate fixation. **Journal of Orthopaedic Surgery**, v.24, n.1, p.97-100, 2016. Available from: <https://doi.org/10.1177/230949901602400122>. Accessed: Dec. 19, 2021. doi: 10.1177/230949901602400122.

ROBERTSON, J. T.; METCALF, H. N. Long-term outcome after implantation of the Prestige I disc in an end-stage indication: 4-year results from a pilot study. **Neurosurgical Focus**, v.17, n.3, p.E10, 2004. Available from: <https://doi.org/10.3171/foc.2004.17.3.10>. Accessed: Dec. 12, 2021. doi: 10.3171/foc.2004.17.3.10.

SEIM, H. B. Cirurgia da Coluna Cervical. In: FOSSUM, T.W. **Cirurgia de Pequenos Animais**. 3 ed. Rio de Janeiro: Elsevier, 2008. Chap 38, p.1402–1459.

SEKHON, L. H. S; BALL, J. R. Artificial cervical disc replacement: principles, types and techniques. **Neurology India**, v.53, n.4, p.445–450, 2005. Available from: <https://doi.org/10.4103/0028-3886.22611>. Accessed: Dec. 12, 2021. doi: 10.4103/0028-3886.22611.

SEKHON, L. H. S. et al. Magnetic resonance imaging clarity of the Bryan, Prodisc-C, Prestige LP, and PCM cervical arthroplasty devices. **Spine**, v.32, n.6, p.673–680, 2007. Available from: <https://doi.org/10.1097/01.brs.0000257547.17822.14>. Accessed: Dec. 12, 2021. doi: 10.1097/01.brs.0000257547.17822.14.

SERTGÖZ, A. Finite element analysis study of the effect of superstructure material on stress distribution in an implant-supported fixed prosthesis. **The International Journal of Prosthodontics**, v.10, n.1, p.19–27, 1997. Available from: <http://www.quintpub.com/userhome/ijp/ijp_10_1_sertgoz_4.pdf>. Accessed: Dec. 12, 2021.

TONIOLLO, M. B. et al. Finite Element Analysis of Bone Stress in the Posterior Mandible Using Regular and Short Implants, in the Same Context, with Splinted and Nonsplinted Prostheses. **The International Journal of Oral & Maxillofacial Implants**, v.32, n4, p.e199- e206, 2017. Available from: <https://doi.org/10.11607/jomi.5611>. Accessed: Jun. 19, 2021. doi: 10.11607/jomi.5611.

TRAYNELIS, V. C. The Prestige cervical disc. **Neurosurgery Clinics of North America**. v.16, n.4, p.621–628, 2005. Available from: <https://doi.org/10.1016/j.nec.2005.06.001>. Accessed: Dec. 12, 2021. doi: 10.1016/j.nec.2005.06.001.

VAN LOON, J.; GOFFIN, J. Unanticipated Outcomes After Cervical Disk Arthroplasty. **Seminars in Spine Surgery**, v.24, n.1, p.20–24, 2012. Available from: <https://doi.org/10.1053/j.semss.2011.11.005>. Accessed: Dec. 12, 2021. doi: 10.1053/j.semss.2011.11.005.

WIGFIELD, C. C. et al. The new Frenchay artificial cervical joint: results from a two-year pilot study. **Spine**, v.27, n.22, p.2446–2452, 2002. Available from: <https://doi.org/10.1097/00007632-200211150-00006>. Accessed: Dec. 12, 2021. doi: 10.1097/00007632-200211150-00006.